Supporting information

A cAMP sensor based on ligand-dependent protein stabilization

Mariapaola Sidoli[1], Ling-chun Chen[2], Alexander J. Lu[2], Thomas J. Wandless[2], William S. Talbot[1*]

[1] Department of Developmental Biology, School of Medicine, Stanford University, Stanford, CA 94305, USA;

[2] Department of Chemical and Systems Biology, School of Medicine, Stanford University, Stanford, CA 94305, USA

* Corresponding author

William Talbot: wtalbot@stanford.edu

Supplementary information includes:

Materials and Methods

Library generation. We implemented a cell-based screening protocol in which AcGFP served as a visual readout for CNBD stability. Random mutations in the cyclic nucleotide-binding domain (CNBD) sequence of MlotiK1 were generated using error-prone PCR [1,2]. To screen for CNBD mutations stabilized by cAMP binding, this library of mutagenized DNA fragments was fused to sequences encoding AcGFP to generate a library of CNBD-GFP fusions expressed from an internal ribosomal entry site. The retroviral expression system pBMN-imCherry was used to stably integrate the library into NIH3T3 cells. A library of 10^4-10^5 members was obtained, and screening was performed as previously described [3].

Cell Culture and flow cytometry. NIH 3T3 cells were cultured and stably transfected as described [3]. For fluorescence detection, transfected NIH 3T3 cells were incubated with 20μM of FSK or 1% serum 17 hours at 30 °C (similar to zebrafish growth conditions) prior to analysis. Cells were trypsinized, resuspended in growth media, and analyzed at the Stanford Shared FACS Facility. 10,000 events were recorded for every sample.

Zebrafish Husbandry. Adult and developing *Danio rerio* zebrafish were maintained at 28 °C, and all the experiments were conducted according to the protocols approved by the Stanford University institutional animal care and use committee and conforming to applicable regulations. Embryos were staged as described [4]. Prior to experimental procedures, embryos and larvae were anesthetized with 0.016% Tricaine. Most experiments were done within the first 24 hours after fertilization; the 8-cpt-cAMP and 8-cpt cGMP treated embryos were imaged between 24-30 hpf, and 1-phenyl 2-thiourea (PTU, 0.003%) was used to inhibit pigmentation. Males and female zebrafish cannot be distinguished at these developmental stages. During DMSO, FSK (Sigma, F6886), 8-cpt-cAMP (BioLog, C010) and 8-cpt-cGMP (sc-202029) treatment, embryos were maintained in E3 embryo medium and were manually dechorionated only when treatments started later than 4 hpf. The *Tg(Gli:mCherry-NLS)* transgenic zebrafish line *Tg(8xGliBS:mCherry-NLS-Odc1)* was kindly provided by James Chen [5].

Cloning and RNA injection. Transcription vectors were generated with restriction cloning by digesting pBMN_N41-GFP and pBMN_N49-GFP with BamH1 and XhoI and assembled in pCS2+ vector with T4 ligase (NEB, M0202). The substitution of arginine to glutamine in position 307 (R307Q) in the N41 and N49 CNBD

sequence was achieved with Q5 site-directed mutagenesis (NEB, E0554) of pMPS8 and pMPS9 respectively, causing AGG>CAG mutations using primers indicated in Table S1. The cAMPr sequence was amplified from p2lox-cAMP (addgene, #99143) [6] and introduced into pCS2+ vector with In-Fusion® HD Cloning Plus (Clontech, 638910). The cilia-localized cAMP sensor was obtained by adding the cilia targeting sequence hARL13b upstream of the sensor; this sequences was amplified from pCS2+8-hARL13b-bPAC-Myc, a gift from Jeremy Reiter [7]. Arl13b-N41-GFP, and the controls Arl13b-N41^{R307Q}-GFP and Arl13b-mApple were assembled with Gibson cloning (NEB, E05510); the primers and plasmid details are available in Table S1 and Table S2. All pCS2+ vectors obtained were digested with MfeI-HF restriction enzyme and transcription was carried out with SP6 polymerase (ThermoFisher/Ambion, am1340). Embryos were injected with 600pg of mRNA of the non-ciliary constructs and 100pg of the ciliary constructs at the one-cell stage.

Generation of Transgenic zebrafish. Stable transgenic lines for *Tg(ubi:N41-GFP)*, *Tg(ubi:N49-GFP), Tg(ubi:N41^{R307Q}-GFP), Tg(ubi:GFP)* and *Tg(ubi:cAMPr)* were created with the *ubi* regulatory element, which was amplified from pDestTol2pA2_ubiC2320_EGFP (addgene #27323) [8] using the primers Ubi_in fus For and Ubi_in fus Rev primers and Herc II polymerase (Agilent, 600675). This fragment was cloned into the pDonP4-P1R vector using In-Fusion (Clontech, 638910). The N41-GFP-polyA, N49-GFP-polyA and N41^{R307Q}-GFP-polyA plasmid DNA were amplified from pMPS8, pMPS9 and pMPS57 respectively using pCR8_CNBD F and pCR8_CNBD R primers and assembled into middle entry clone pCR8 with TA cloning (ThermoFisher, K252002). For *Tg(ubi:GFP)* and *Tg(ubi:cAMPr)* the GFP and cAMPr sequences were amplified from pMPS9 and pMPS66 respectively and cloned into pCR8 with In Fusion cloning. LR clonase II (ThermoFisher, 12538120) was used to assemble the Gateway compatible vectors into pDest_Tol2 containing the upstream regulatory *ubi* region, the middle entry clones and the 3' Entry clone pDonP2R-P3 SV40-pA (pAMS111). For *Tg(ubi:N41^{R307Q}-GFP)* the TOL2 vector included cmlc2:mCherry sequence downstream as selection marker. The resulting TOL2 plasmids for ubi:N41-GFP, ubi:N49-GFP, ubi:N41^{R307Q}-GFP, ubi:GFP and ubi:cAMPr were co-injected into one-cell stage embryos with 30ng/μl of transposase mRNA [9,10]. Embryos were screened for GFP signal at 24 hpf (or red heart at 48 hpf; cmlc2:mCherry) and raised to adulthood (Figure S2A; lower diagram). Details on primers and plasmids are available in Table S1 and Table S2.

Generation of GPR161 CRISPR mutants. sgRNAs targeting *gpr161a,* and *gpr161b* are reported in Table S1 and were designed using CHOPCHOP (https://chopchop.cbu.uib.no/) [11,12] . A 120 bp DNA fragment containing the T7 binding site sequence, the targeting sequence and tracrRNA were transcribed into sgRNA using HiScribe T7 Quick (NEB, E2050S) kit for 16 hours at 37 ºC. RNA was purified using mirVana miRNA isolation kit (Invitrogen, AM1561), quantified using NanoDrop 8000 and quality checked on a 2% agarose gel. CRISPR injections were performed at 1-cell stage. CRISPR-Cas9 injection solution consisted of 300ng/µl of sgRNA was mixed with 300 ng/µl of Cas9 protein (Macrolab, Berkeley, http://qb3.berkeley.edu/macrolab/cas9-nls-purified-protein/) in Tris-HCl (pH 7.5). Between 300-600 pg of sgRNA were injected in one-cell stage wild type embryos and surviving fish were raised to adulthood. To test for germline transmission, adults were outcrossed with wildtype fish and screened for frameshift indels. The *gpr161a st129* mutation contains an indel in exon 2 (-6+4 bp), whereas *the gpr161b* allele *st128* contains an 8-bp deletion in exon2. Details of the targeting sequence, the genotyping primers and restriction enzymes are described in Table S1.

In situ hybridization. Antisense probe for *gfp* was generated by amplifying 680 bp of *gfp* DNA from pCS2+-N41-acGFP (pMPS8) and inserting it into pCRII-TOPO (ThermoFisher, K4600-40). Primers details are available in Table S1. *In situ* hybridization for *gfp* mRNA in whole-mount 24 hpf embryos was performed using standard methods [13] with minor modifications. In brief, embryos were dechorionated and fixed with 4% paraformaldehyde overnight at 4°C. Embryos were dehydrated with 5 washings (2 minutes each) of 100% methanol. After PBS-Triton X-100 washings, embryos were permeabilized with 1/2000 dilution of protein K (20 mg/ml) for 10 minutes and incubated overnight with 1/100 dilution of GFP riboprobes at 65 ºC. After incubation with 1/3000 of anti-digoxigenin antibody conjugated to alkaline phosphatase in MAB block embryos were let in developing buffer with NBT (Roche, 11383213001) and BCIP (Roche, 11383221001) substrates for 30 minutes at least and the state of colorimetric assay was checked every 5 minutes.

Whole Embryo, somite and EVL imaging. Embryos were dechorionated, if not previously done before imaging, and immobilized in 1.5% agarose or in 0.3% agarose (for time lapse) in E3 1X and 0.016% Tricaine. Whole embryos were imaged under Zeiss LSM700 confocal microscope with a 10x objective. Somite imaging was done using 20x objectives in experiments involving FSK treatment, whereas the analyses in EVLs and *gpr161* mutants was carried out under a 40x water immersion objective. Time lapse images were performed with a Zeiss LSM700

confocal microscope using 10x or Zeiss LSM980 with Airyscan 2 Confocal Microscope using 25x silicone immersion. Cilia were also imaged using Zeiss LSM980 with Airyscan 2 Confocal Microscope using 25x silicone immersion. The levels for laser power and gain were set to optimize images for the FSK and 8-cpt-cAMP treated embryos to avoid oversaturation. The analyses of fluorescence intensity were performed on maximum intensity projections containing the same number of focal planes in all the conditions or genotype groups. All images in each experiment were acquired and compared under the same conditions, and they were analyzed in their original form, with no post-acquisition processing. For the analyses in the somites and EVL, identical ROIs were designed to surround the proper areas to quantify and areas containing background. The pixel value of background was manually subtracted from the pixel value of the ROI. For the analyses in whole embryos and cilia, the fluorescence intensity was performed using a thresholding script in Fiji.

Statistical analysis. All statistical analysis was conducted using Graph pad Prism 6.01. Normality and lognormality test was performed using D'Agostino & Pearson, Anderson-Darling, Shapiro-Wilk and Kolmogorov-Smirnov tests. Where the raw data set was not normal, log10 transformation was carried out. The significance among groups was determined using Student's *t* test, one-way and two-way ANOVA. $P \leq 0.05$ was considered statistically significant. Graphical data are represented as mean ± SD (standard error) or SEM (standard error of the mean).

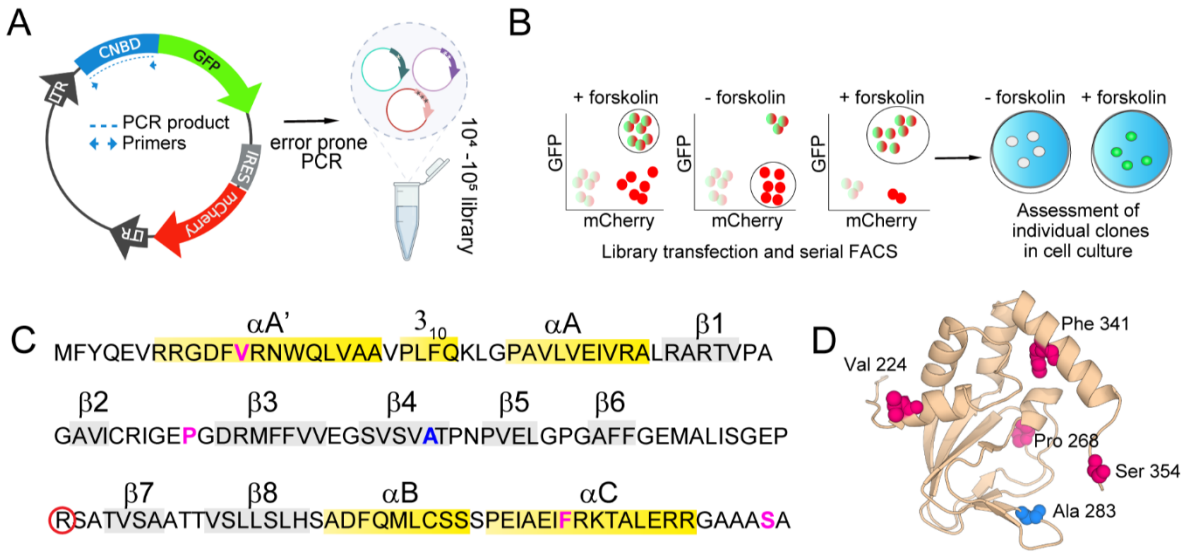

Figure S1. Selection of CNBD variants. **(A)** Scheme representing the use of error-prone PCR to construct library of cyclic nucleotide binding domain (CNBD) mutants in retrovirus-based expression vector. mCherry protein, expressed via IRES was used as a transfection efficiency control. **(B)** Clones expressing library of mutant CNBDs were selected using fluorescence monitored by analytical flow cytometry for cells with high GFP expression in the presence of forskolin and low GFP expression in the absence of forskolin. **(C)** Coding sequence of the CNBD from MlotiK1, noting structural features including alpha-helices (yellow), beta-sheets (grey). A conserved Arg residue (R) that is essential for cAMP binding is circled in red; we mutated this residue to create the negative control for the sensor (R307Q). Residues altered in two candidate cAMP sensors are shown in blue and magenta; sensor N49 has a single nucleotide change (blue), whereas sensor N41 has 4 separate missense mutations (magenta). **(D)** Ribbon diagram of the CNBD peptide (PBD:2KXL) [14,15], where the mutations are highlighted in the structure as blue spheres for N49 variant and as magenta spheres for N41.

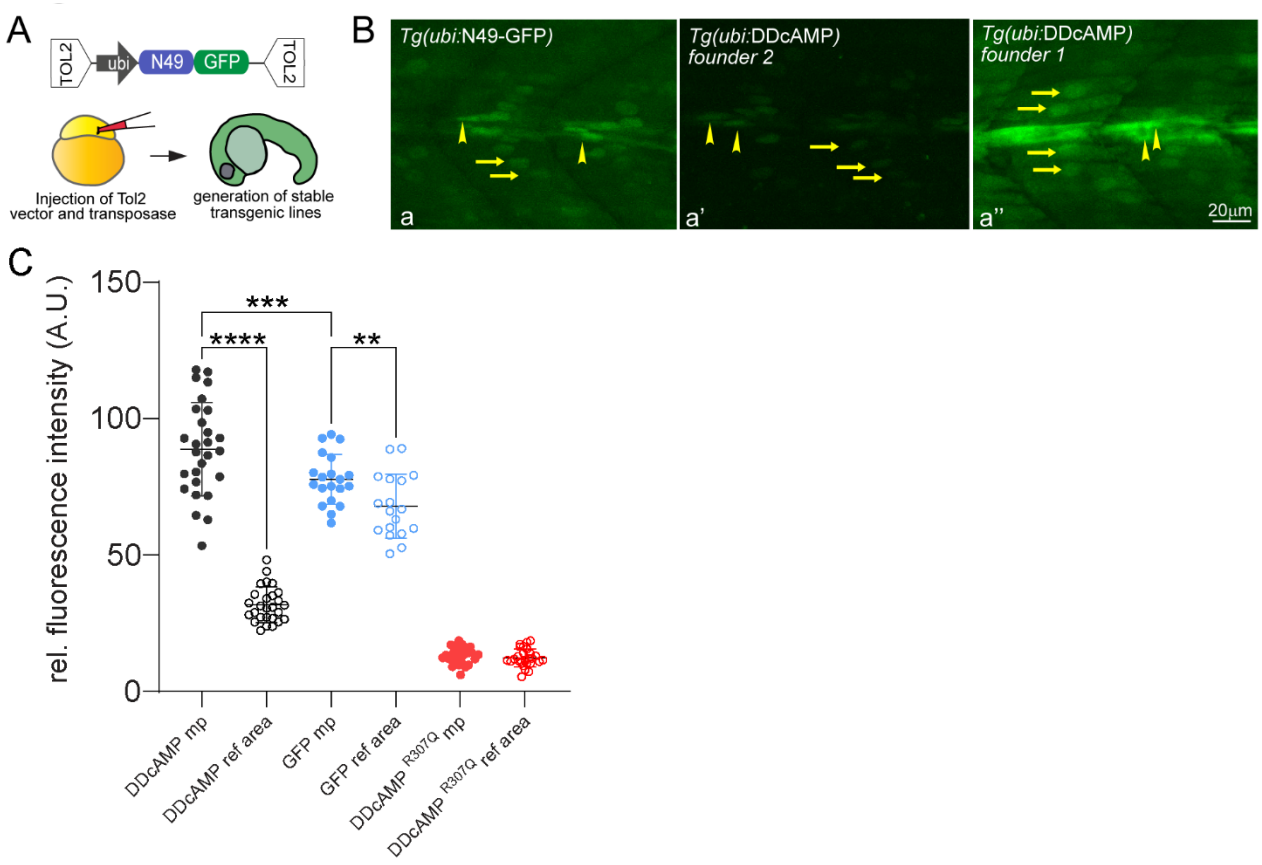

Figure S2. GFP labels muscle pioneers and slow superficial fibers. **(A)** Upper panel: Diagram of the TOL2 plasmids containing N49-GFP and *ubi* regulatory sequences. Lower panel: Scheme of one-cell stage injection to raise adult fish injected with the TOL2 plasmid and transposase. Adults were screened and crossed to generate stable transgenic lines**.** **(B)** Magnified view of somites, showing muscle pioneers (arrowheads) and superficial slow fibers (arrows). **(C)** quantification of the fluorescence intensity in the area of the strongly expressing muscle pioneers (mp) and in a region of the animal not containing muscle pioneers (ref area) from Tg(Ubi:DDcAMP), Tg(Ubi:GFP) and Tg(Ubi:DDcAMP^{R307Q}) embryos shown Figure 2. Error bars, SD: **p<0,01; ***p<0,001; ****p<0,0001 by One-way ANOVA (Šídák's multiple comparisons), n=25-30. A.U. = arbitrary unit.

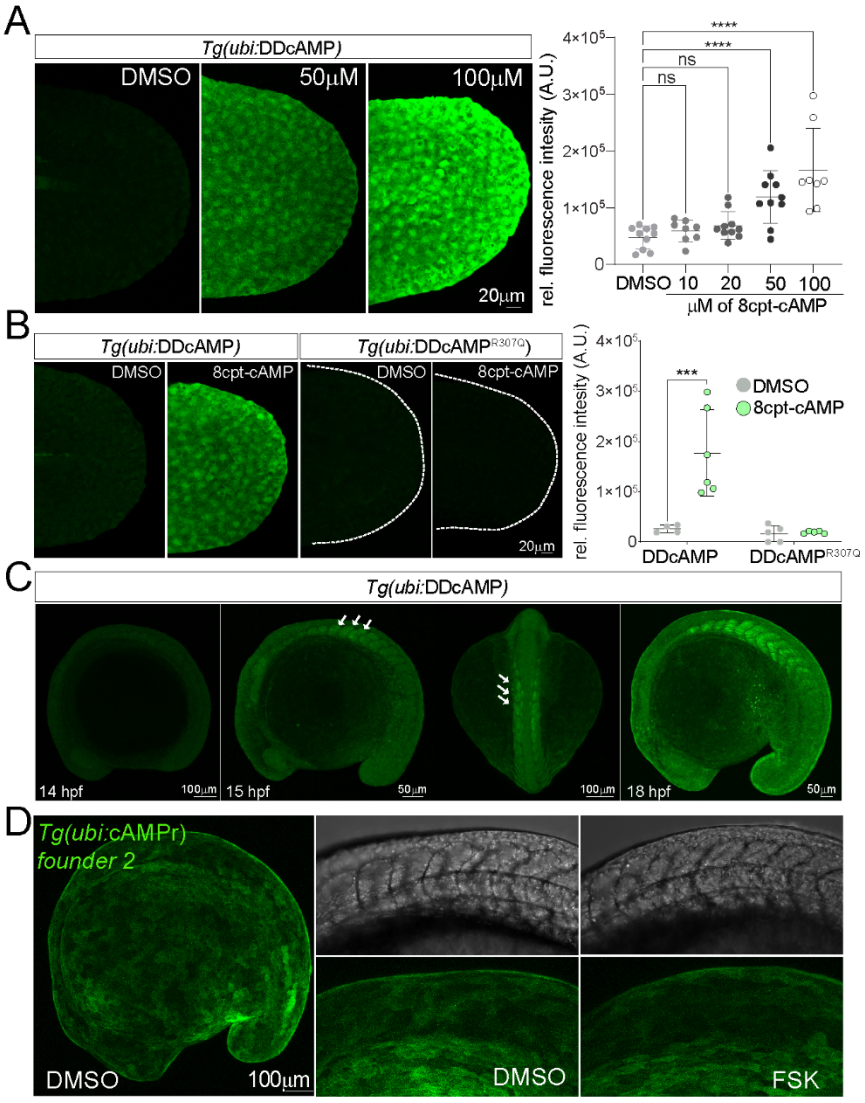

Figure S3. DDcAMP is sensitive and specific to cAMP. **(A)** *Tg(ubi:*DDcAMP*)* embryos from the same clutch were treated with DMSO or 10μM, 20μM, 50μM, 100μM 8-cpt-cAMP for 24 h. GFP in twenty EVL cells was quantified, and the fluorescence intensity in each animal was averaged. Each point represents a single animal. Error bars, SD; ****p<0.0001 one-way ANOVA (with Dunnet's comparisons), n=9-10 animals per condition, ns = not significant. A.U. = arbitrary unit. **(B)** 12-13 somite stage embryos with *Tg(ubi:*DDcAMP*)* or *Tg(ubi:* DDcAMP ^{R307Q}*)* transgene were treated with 1 mM 8-cpt-cAMP for 24 hours, GFP in EVL cells was quantified as previously described. Error bars, SD: ***p<0,001 by Two-way ANOVA (Šídák's multiple comparisons), n=4-6. A.U. = arbitrary unit. **(C)** Time course of *Tg(ubi:*DDcAMP*)* at 14 hpf, 15 hpf and 18 hpf shows a gradual increase of GFP intensity during somite development, starting in anterior somites (white arrows). **(D)** Confocal images of *Tg(ubi:*cAMPr*)* embryos at 16 hpf from founder 2, and magnification of the somites after 2 hours of DMSO or FSK treatment.

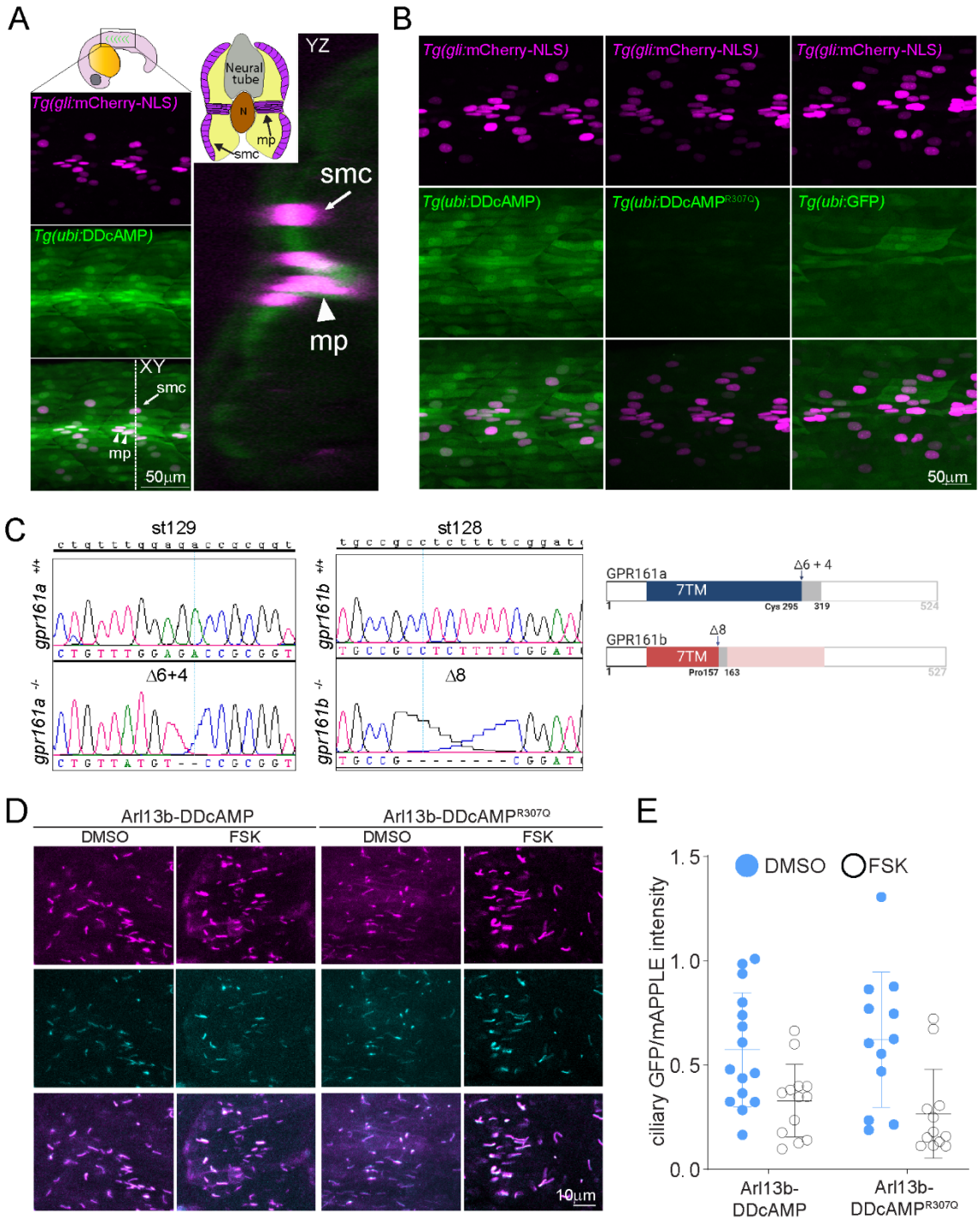

Figure S4. DDcAMP labels cells responsive to Shh. **(A)** Confocal images (Airyscan 2 processing) of somites from 24 hpf embryos expressing *Tg(ubi:*DDcAMP*)* to detect cAMP (green) and *Tg (Gli:*mCherry-NLS*)* to reveal Shh signaling activity via nuclear label of Gli activity (magenta). cAMP signal is detected in slow muscle cells (smc, white arrows) and muscle pioneers (mp, white arrowheads), which are responsive to Shh signal (XY and YZ orthogonal views). N= notochord. **(B)** Confocal images showing cAMP (green) in cells responsive to Shh signal

(magenta) in *Tg(ubi:*DDcAMP*)* muscle cells but not in muscle cells of embryos harboring the *Tg(ubi:*DDcAMP^{R307Q}*)* and *Tg(ubi:*GFP*)* transgenes. **(C)** Left: sequence characterization of mutations generated with CRISPR-Cas9 in *gpr161a* and *gpr161b* genes. Right: protein diagram showing the first and last amino acids, the last amino acid in frame, the position of the stop codon and the 7TM (7 transmembrane domains) of Gpr161a (blue) and Gpr161b (red). The indel in Gpr161a generates a premature stop codon in position 319 of TMD-7 while the deletion in Gpr161b generates a premature stop codon in position 163 in the TMD-4. **(D)** Confocal image of somites in 24 hpf embryos co-injected with synthetic RNA to label cilia (Arl13b-mApple, top row) and (middle row) the ciliary variants of DDcAMP (Arl13b-DDcAMP) or control DDcAMP (Arl13b-DDcAMP^{R307Q}), after 20 hours of DMSO or 20μM FSK treatment. **(E)** GFP and mApple intensities were quantified after Arl13b-DDcAMP and Arl13b-DDcAMP^{R307Q} mRNA injection and 20 hours of DMSO or FSK treatment. Each dot represents the average of the ratio between GFP and mApple intensities in each single embryo. Error bar; SD. FSK treatment did not significantly change the signal from either ciliary DDcAMP or ciliary control DDcAMP^{R307Q}.

References

(1) Banaszynski, L. A.; Chen, L.-C.; Maynard-Smith, L. A.; Ooi, A. G. L.; Wandless, T. J. A Rapid, Reversible, and Tunable Method to Regulate Protein Function in Living Cells Using Synthetic Small Molecules. *Cell* **2006**, *126* (5), 995–1004. https://doi.org/10.1016/j.cell.2006.07.025.

(2) McCullum, E. O.; Williams, B. A. R.; Zhang, J.; Chaput, J. C. Random Mutagenesis by Error-Prone PCR. In *In Vitro Mutagenesis Protocols: Third Edition*; Braman, J., Ed.; Methods in Molecular Biology; Humana Press: Totowa, NJ, 2010; pp 103–109. https://doi.org/10.1007/978-1-60761-652-8_7.

(3) Navarro, R.; Chen, L.-C.; Rakhit, R.; Wandless, T. J. A Novel Destabilizing Domain Based on a Small-Molecule Dependent Fluorophore. *ACS Chem Biol* **2016**, *11* (8), 2101–2104. https://doi.org/10.1021/acschembio.6b00234.

(4) Kimmel, C. B.; Ballard, W. W.; Kimmel, S. R.; Ullmann, B.; Schilling, T. F. Stages of Embryonic Development of the Zebrafish. *Developmental Dynamics* **1995**, *203* (3), 253–310. https://doi.org/10.1002/aja.1002030302.

(5) Mich, J. K.; Payumo, A. Y.; Rack, P. G.; Chen, J. K. In Vivo Imaging of Hedgehog Pathway Activation with a Nuclear Fluorescent Reporter. *PLoS One* **2014**, *9* (7). https://doi.org/10.1371/journal.pone.0103661.

(6) Hackley, C. R.; Mazzoni, E. O.; Blau, J. CAMPr: A Single-Wavelength Fluorescent Sensor for Cyclic AMP. *Sci. Signal.* **2018**, *11* (520). https://doi.org/10.1126/scisignal.aah3738.

(7) Truong, M. E.; Bilekova, S.; Choksi, S. P.; Li, W.; Bugaj, L. J.; Xu, K.; Reiter, J. F. Vertebrate Cells Differentially Interpret Ciliary and Extraciliary CAMP. *Cell* **2021**, *184* (11), 2911-2926.e18. https://doi.org/10.1016/j.cell.2021.04.002.

(8) Mosimann, C.; Kaufman, C. K.; Li, P.; Pugach, E. K.; Tamplin, O. J.; Zon, L. I. Ubiquitous Transgene Expression and Cre-Based Recombination Driven by the Ubiquitin Promoter in Zebrafish. *Development* **2011**, *138* (1), 169–177. https://doi.org/10.1242/dev.059345.

(9) Kawakami, K. Tol2: A Versatile Gene Transfer Vector in Vertebrates. *Genome Biol* **2007**, *8* (Suppl 1), S7. https://doi.org/10.1186/gb-2007-8-s1-s7.

(10) Suster, M. L.; Kikuta, H.; Urasaki, A.; Asakawa, K.; Kawakami, K. Transgenesis in Zebrafish with the Tol2 Transposon System. *Methods Mol Biol* **2009**, *561*, 41–63. https://doi.org/10.1007/978-1-60327-019-9_3.

(11) Montague, T. G.; Cruz, J. M.; Gagnon, J. A.; Church, G. M.; Valen, E. CHOPCHOP: A CRISPR/Cas9 and TALEN Web Tool for Genome Editing. *Nucleic Acids Res* **2014**, *42* (W1), W401–W407. https://doi.org/10.1093/nar/gku410.

(12) Labun, K.; Montague, T. G.; Gagnon, J. A.; Thyme, S. B.; Valen, E. CHOPCHOP v2: A Web Tool for the next Generation of CRISPR Genome Engineering. *Nucleic Acids Res* **2016**, *44* (W1), W272–W276. https://doi.org/10.1093/nar/gkw398.

(13) Lyons, D. A.; Pogoda, H.-M.; Voas, M. G.; Woods, I. G.; Diamond, B.; Nix, R.; Arana, N.; Jacobs, J.; Talbot, W. S. Erbb3 and Erbb2 Are Essential for Schwann Cell Migration and Myelination in Zebrafish. *Curr. Biol.* **2005**, *15* (6), 513–524. https://doi.org/10.1016/j.cub.2005.02.030.

(14) Clayton, G. M.; Silverman, W. R.; Heginbotham, L.; Morais-Cabral, J. H. Structural Basis of Ligand Activation in a Cyclic Nucleotide Regulated Potassium Channel. *Cell* **2004**, *119* (5), 615–627. https://doi.org/10.1016/j.cell.2004.10.030.

(15) Schünke, S.; Stoldt, M.; Lecher, J.; Kaupp, U. B.; Willbold, D. Structural Insights into Conformational Changes of a Cyclic Nucleotide-Binding Domain in Solution from Mesorhizobium Loti K1 Channel. *PNAS* **2011**, *108* (15), 6121–6126. https://doi.org/10.1073/pnas.1015890108.